Supplementary Information

Hongchuan Shen[1], Peng Tan[1,2*] and Lei Xu[1*]

[1]*Department of Physics, The Chinese University of Hong Kong, Hong Kong, China*

[2] *State Key Laboratory of Surface Physics, Department of Physics,*

Fudan University, Shanghai 200433, China

(Dated: December 14, 2015)

I. Experimental details and covariance matrix analysis

Our system is constructed by self-propelled active particles confined in a 2D square lattice. Our particles are identical metal spheres with $d = 13.00 \pm 0.01mm$ and $m = 9.915 \pm 0.005g$(the total mass of one sphere plus one motor). Each particle is connected to four nearest neighbors by identical springs ($k = 2.97 \pm 0.16N/m$, $l_0 = 15.46 \pm 0.36mm$) and form a square lattice as shown in Fig.1a. All springs are stretched to reach the lattice constant of $45.0 \pm 1.5mm$ and the entire system contains $15 \times 15 = 225$ particles. To control the mobility at single-particle level, under *every* particle we attach a small vibrating motor independently driven by external power input. Once turned on, motors will drive particles to move randomly around their equilibrium positions in 2D (see the supplemental movie).

Since the attractive interaction between particles is harmonic, the spatial fluctuations (renormalized by local variance) obey an excellent Gaussian distribution as shown in Fig.1b. Clearly every particle has a well-defined equilibrium position, and the time-averaged deviation from it, $\langle \delta r_i \rangle = \langle \sqrt{\delta x_i^2 + \delta y_i^2} \rangle$, provides a good description for the mobility of each particle. We measure the local displacements by tracking the center of every particle and obtain their x and y coordinates with respect to time. We then calculate the average position of every particle and the displacement δr_i is calculated as the deviation from the average position. $\langle \delta r_i \rangle$ is then calculated from the average of all frames.

The mobility of one typical particle versus time is shown in Fig.SI-1, and the three curves

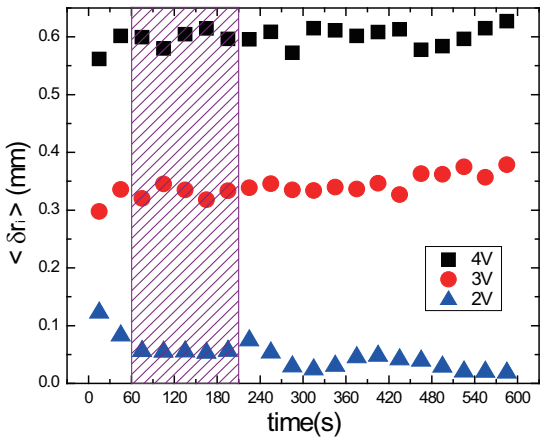

FIG. SI - 1. The persistence of mobility levels for one typical motor under three driving voltages. The shaded area is the measurement period.

correspond to three typical driving voltages. We choose a stable period to perform measurements, as labeled by the shaded area. We determine the particle location uncertainties by measuring a static sample and calculating the fluctuations of the static particles under the exact condition of a real experiment. We find the uncertainty of $\langle \delta r_i \rangle$'s to be $0.007mm$. Since the small $\langle \delta r_i \rangle$ values only affect the high-$\hat{\omega}$ region, which are systematically measured in Fig.5, we make sure that the smallest $\langle \delta r_i \rangle$ there is $0.064mm \gg 0.007mm$, and thus the uncertainty is much smaller than the real movement and can be safely neglected.

With the data from particle tracking, we can construct the covariance matrix of spatial fluctuations and calculate its eigenmodes [16, 35, 36]. More specifically, we track the positions of all particles for 1250 frames and construct the covariance matrix [16, 35, 36]: $C_{i,j} = \langle [\boldsymbol{r}_i(t) - \langle \boldsymbol{r}_i(t) \rangle][\boldsymbol{r}_j(t) - \langle \boldsymbol{r}_j(t) \rangle] \rangle$, with $i, j = 1, ..., 2N_p$ running over the x and y coordinates of all particles, and $\langle\rangle$ indicating time average over all frames. To eliminate the boundary effect, we only use the central $N_p = 11 \times 11 = 121$ particles which result in $2N_p = 242$ eigenmodes. In equilibrium systems, these eigenmodes are identical to the vibrational modes, with the eigenvalue λ directly related to the vibrational frequency ω: $\omega \propto 1/\sqrt{\lambda}$. Analogous to ω, therefore, in our non-equilibrium system we define a dimensionless parameter, $\hat{\omega} \equiv \langle \overline{\delta r} \rangle / \sqrt{\lambda}$, which has the same λ dependence and renormalized by the time-and-location averaged displacement $\langle \overline{\delta r} \rangle$. Due to the lack of equipartition, our eigenmodes are *not* equivalent to vibrational modes anymore, but they still indicate specific patterns of collective movements (see Fig.2a), following which the system can achieve the overall displacements described by $\sqrt{\lambda}$ or $1/\hat{\omega}$.

We then determine the density of states $D(\hat{\omega})$ by finding the distribution of $\hat{\omega}$ with the commonly-used linear binning. We carefully choose the bin width to ensure enough statistics in most bins (typically more than 4 or 5), and when the bin width is slightly varied our data remain stable.

II. The statistics analysis

In our covariance matrix [16, 35, 36] calculations the degrees of freedom is $N = 242$ and we take the statistics over $T = 1250$ frames. According to previous studies [35], the number of frames must be significantly larger than the degrees of freedom. To determine whether our statistics is good enough, we compare our measurements with Ref.[35]. As pointed out by Ref. [35], the ratio, N/T, is the essential parameter determining whether the statistics is good enough: the smaller N/T

is, the better the statistics is. For example, in Ref. [35] the sample contains 3600 particles, and the measurement with the best statistics was achieved by taking T = 30000 frames of pictures, which makes $N/T = 2 * 3600/30000 = 0.24$. In our experiment, because of the relatively small number of particles we used ($N_p = 121$), the degrees of freedom is also small ($N = 2 * N_p = 242$). Therefore, using $T = 1250$ frames of images already achieves a very small ratio of N/T = 0.19, which is even better than the best situation in Ref. [35] (i.e., N/T = 0.24 there).

Moreover, to accurately quantify the errors caused by the statistics, we performed a new set of measurements and increased the frame number by one order of magnitude to $T_{max} = 12955$. With this new set of experiment, we can study the influence of T values in the range of $T = 1250 - 12955$ frames. According to Ref.[17], the ratio N/T mainly affects the spectrum by changing the values of $\hat{\omega}$ in the high-$\hat{\omega}$ regime, while making very little influence to the low-$\hat{\omega}$ modes. Here we plot our measurements in Fig.SI-2: the left panel shows three typical low-$\hat{\omega}$ modes (m1, m4, m6) and the right panel plots three typical high-$\hat{\omega}$ modes (m237, m240, m242).

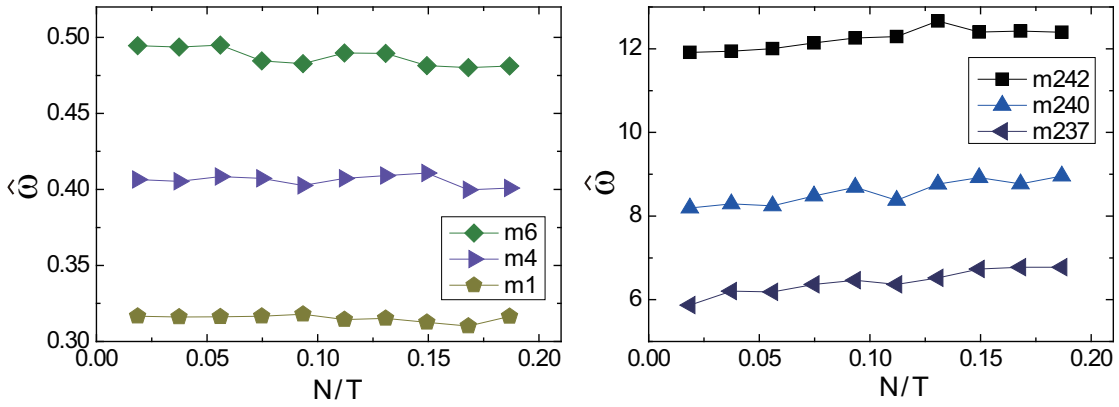

FIG. SI - 2. The influence of statistics. We increase the frame number T up to $T_{max} = 12955$, and keep the degrees of freedom $N = 242$ constant. The left panel shows three typical low-$\hat{\omega}$ modes, and the right panel shows three high-$\hat{\omega}$ modes.

Clearly, as N/T decreases with the increase in T, the left panel shows very little variation, with the values of $\hat{\omega}$ changing within 3%. For the high-$\hat{\omega}$ modes in the right panel, however, we observe a small-slope linear dependence, and the $\hat{\omega}$ values vary around 10%. All these results are in great agreement with Ref.[17]. Therefore, in the low-$\hat{\omega}$ regime all our discussions on the boson peak formation should be quantitatively valid within 3% of uncertainty; while there may exist errors around 10% in the high-$\hat{\omega}$ region, which however should not affect the qualitative conclusions we

have drawn there.

III. Restore to the Debye behavior from boson peak spectrum

To completely confirm that the boson peak in samples C and D are indeed caused by the large-activity particles, we tune these active particles back to normal activity, and measure the reduced density of states as shown in Fig.SI-3. As we expect, the $D(\hat{\omega})/\hat{\omega}$ spectra return back to the flat Debye-like behavior! This experiment unambiguously verified that the boson peak is indeed caused by the active particles and when they are turned back to normal the peak also goes away.

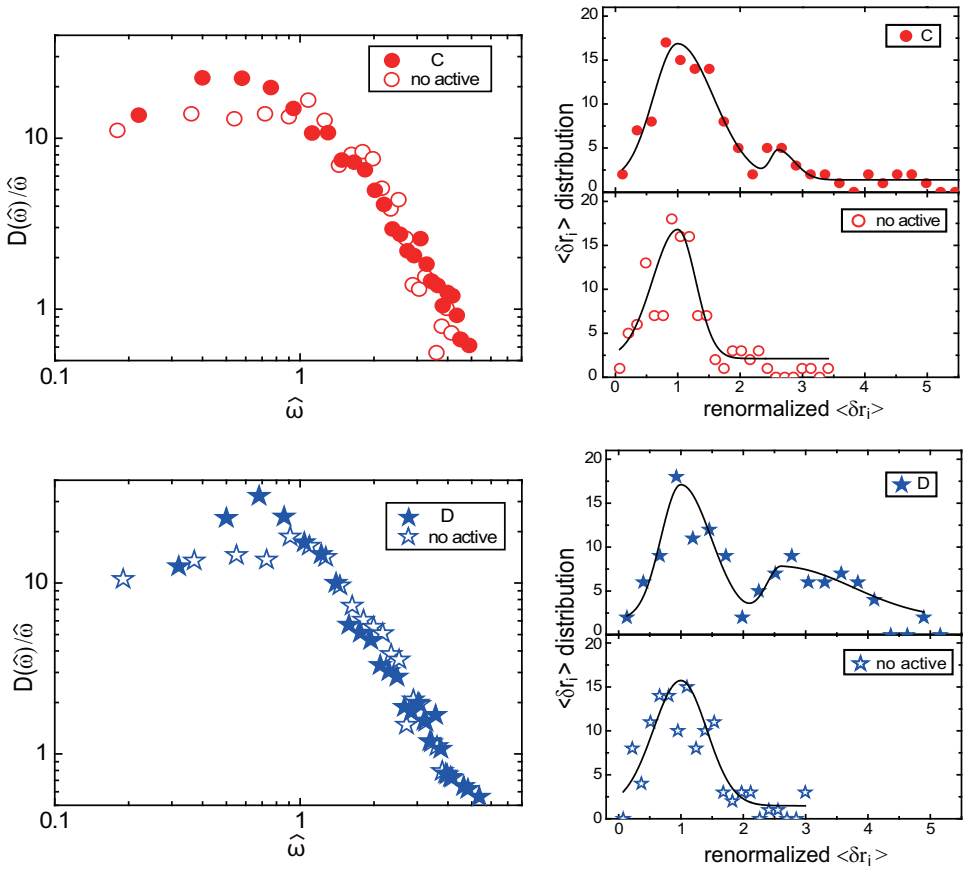

FIG. SI - 3. The restoring of the Debye behavior in samples C and D. As we tune the active particles to normal activity in C and D, boson peak disappears and the Debye behavior is re-established.

IV. More data with inactive particles

As shown in Fig.5c, it seems that inactive particles also reduce the participation ratio in low-

$\hat{\omega}$ region. However, here we show that there is no consistent trend in the low-$\hat{\omega}$ region. In two different samples demonstrated in Fig.SI-4, the participation ratio does not always decrease in the low-$\hat{\omega}$ region, and in some places it even increases. Therefore, by combining all the results we have, the only conclusion we can make is that at high-$\hat{\omega}$ region the participation ratio decreases with N_i, while no conclusive conclusion can be drawn in the low-$\hat{\omega}$ region.

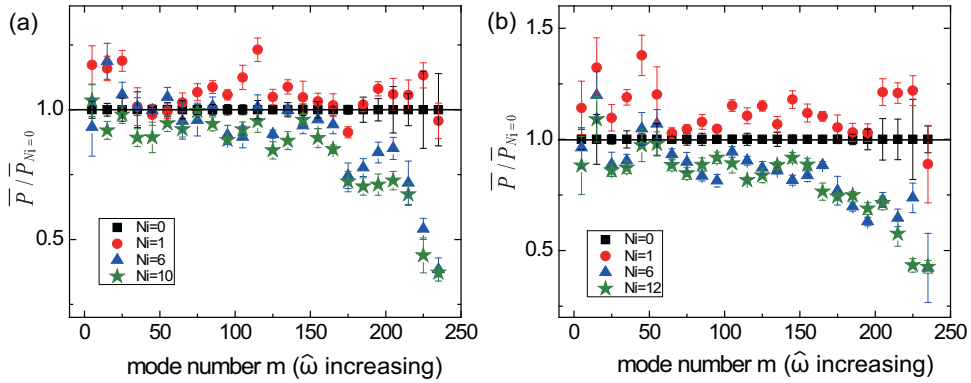

FIG. SI - 4. More data sets for the influence of inactive particles to the high-$\hat{\omega}$ region. The two samples are different from the one shown in Fig.5c and they again show a decrease in high-$\hat{\omega}$ region. However there is no consistent trend in the low-$\hat{\omega}$ region.

V. Projection of the real displacement field onto the modes

To further probe the relation between the real dynamics and the modes. We project the real displacement field onto the modes in Fig.SI-5, for three different time delays. Here $\Sigma|C_m|^2$ is the cumulative projection probabilities and m is the mode number, running from low to high $\hat{\omega}$. Different curves correspond to different time delays during which the real displacement field is measured, and we use the number of frames T to label the time delay. Clearly as the time interval increases, the low-$\hat{\omega}$ modes become more and more important for the real displacement, indicating that low-$\hat{\omega}$ does correspond to long time interval. This is similar to the relation between real displacements and the vibrational modes in equilibrium systems. Therefore, the modes from covariance matrix [16, 35, 36] in non-equilibrium systems do seem to relate to real displacements and this phenomenon raises an intriguing question asking for further study.

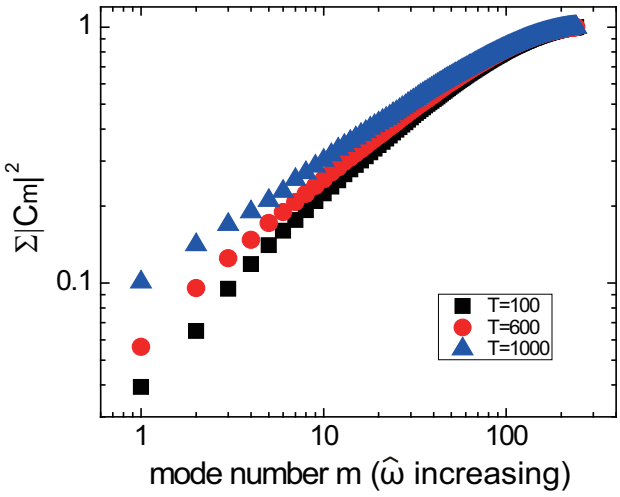

FIG. SI - 5. Projecting real displacement with different time delays onto the modes. $\Sigma|C_m|^2$ is the cumulative projection probabilities and m is the mode number, running from low to high $\hat{\omega}$. The time delay is labeled by the number of frames T.